Published in final edited form as:

*Comput Methods Biomech Biomed Engin*. 2015 ; 18(3): 332–337. doi:10.1080/10255842.2013.794898.

# Mechanical evaluation of a tissue-engineered zone of calcification in a bone–hydrogel osteochondral construct

**Jérôme Hollenstein**[a,b], **Alexandre Terrier**[a], **Esther Cory**[b], **Albert C. Chen**[b], **Robert L. Sah**[b,c], and **Dominique P. Pioletti**[a,*]

[a]Laboratory of Biomechanical Orthopedics, Institute of Bioengineering, Ecole Polytechnique Fédérale de Lausanne (EPFL), CH-1015 Lausanne, Switzerland [b]Department of Bioengineering, University of California – San Diego (UCSD), 9500 Gilman Drive, La Jolla, CA 92093, USA [c]Department of Orthopaedic Surgery, University of California – San Diego (UCSD), 9500 Gilman Drive, La Jolla, CA 92093, USA

## Abstract

The objective of this study was to test the hypothesis that mechanical properties of artificial osteochondral constructs can be improved by a tissue-engineered zone of calcification (teZCC) at the bone–hydrogel interface. Experimental push-off tests were performed on osteochondral constructs with or without a teZCC. In parallel, a numerical model of the osteochondral defect treatment was developed and validated against experimental results. Experimental results showed that the shear strength at the bone–hydrogel interface increased by 100% with the teZCC. Numerical predictions of the osteochondral defect treatment showed that the shear stress at the bone–hydrogel interface was reduced with the teZCC. We conclude that a teZCC in osteochondral constructs can provide two improvements. First, it increases the strength of the bone–hydrogel interface and second, it reduces the stress at this interface.

### Keywords

interfacial tissue engineering; osteochondral defect; push-off test; calcification

## 1. Introduction

A zone of calcified cartilage links the hyaline cartilage to bone. This calcified interface functions as a mechanical transition conferring an intermediate stiffness between that of soft tissue and bone (Redler et al. 1975; Broom et al. 1996; Ferguson et al. 2003; Hauch et al. 2009). Indeed, a gradient in mechanical properties in soft structure helps reducing stress accumulation at the interface with a stiffer material (Yang and Temenoff 2009). The zone of calcified cartilage also protects hyaline cartilage from passive mineralisation (Oegema et al. 1997).

*Corresponding author. dominique.pioletti@epfl.ch.

The importance of a calcified zone for the anchorage of cartilage was demonstrated *in vitro* with porous calcium polyphosphate substrate (Allan et al. 2007; St-Pierre et al. 2012). The control of a tissue-engineered zone of calcification (teZCC) may present a biomechanical advantage in the development of artificial osteochondral constructs (St-Pierre et al. 2010). However, such a calcified interface is not often created during osteochondral tissue engineering (Schaefer et al. 2002; Emans et al. 2005; Lima et al. 2008; Grayson et al. 2010).

In experimentally developing an artificial osteochondral construct incorporating a teZCC, a biomechanical analysis should be performed to address its biomechanical effect. In particular, the anchorage aspect between the hydrogel-like material and the bone-like material should be evaluated, such as in the context of an osteochondral defect treatment. As no such evaluation could be found in the literature, the purpose of this study was to test the potential mechanical advantage of a teZCC for an artificial osteochondral construct. In parallel, an experimental double-diffusion system was used to obtain a teZCC at the interface between a hydrogel and a trabecular bone. The experimental mechanical tests performed on these osteochondral constructs were used to validate the numerical model.

## 2. Materials and methods

### 2.1 Study design

A mixed experimental–numerical analysis was designed to evaluate the potential mechanical advantage of a teZCC for the anchorage of a hydrogel on a trabecular bone. A numerical knee model was developed to evaluate the mechanical behaviour of an osteochondral construct with or without teZCC placed in a simulated knee cartilage defect. In parallel, teZCC was experimentally obtained with a double diffusion system. Push-off tests were performed to evaluate the anchorage performance of the obtained osteochondral construct. Finally, the push-off tests were numerically replicated and experimental/numerical results were confronted for validating the numerical model of the teZCC.

### 2.2 Numerical osteochondral defect model

The numerical model represented an osteochondral defect treatment in a 2D axisymmetric model for a tibio-femoral joint (Figure 1(A)). The osteochondral construct had a diameter of 6 mm and was composed of trabecular bone and hydrogel both 3 mm thick. The teZCC was either 0 (no teZCC) or 0.5 mm thick. Materials described in Figure 1 were assumed homogenous and isotropic. The bone, ZCC and teZCC were considered linear elastic, whereas the cartilage and hydrogel were described by Neo-Hookean laws as suggested in previous studies (Butz et al. 2011; Wiltsey et al. 2013). The elastic moduli $E$ of the agarose hydrogel and the calcified hydrogel (teZCC) were set to 0.16 and 1.5 MPa, respectively (Hollenstein et al. 2011). All materials properties are summarised in Table 1. No contact was considered. The construct was aligned to the cartilage (bottom of hydrogel aligned with the bottom of the host cartilage) to match the host tissue layers (Figure 1(A)). The left edge of the model was the symmetrical axis, while the right edge was unconstrained. The bottom edge was fixed. A 30% deformation to the opposing host cartilage (zone 5) was applied from the top (Figure 1(A)). It induced a 10% deformation of the host cartilage (zone 6). The maximal shear stress at the construct hydrogel– teZCC interface was calculated. The

numerical model was solved by Comsol 4.2 (COMSOL, Burlington, MA, USA) with MUMPS solver and quadratic triangles elements, physically control by Comsol and set as 'extremely fine'.

## 2.3 Experimental setup and numerical validation

**2.3.1 Bone sample preparation—**Trabecular bone samples were harvested from adult bovine condyle. Blocks were cut off from lateral and medial condyle using bone saw and drill press with 6 mm diameter coring bit. Using an Isomet low speed bone saw, the subchondral bone was removed. The bone was cut in order to get a thickness of 3 mm. A sonicator and a water pick were used to remove the bone marrow and debris. The samples were finally soaked in oxygen peroxide overnight. Samples were stored at −20°C.

**2.3.2 Double diffusion system—**A system was built to allow solutes of two different solutions, calcium chloride and sodium phosphate, to diffuse towards each other within agarose hydrogel, as described previously (Boskey 1989; Hollenstein et al. 2011). Solutions were of 100 mM and buffered with 150 mM HEPES at pH 7.4. Trabecular bone disks, as prepared in Section 2.3.1, were infiltrated within a 2% agarose hydrogel (SeaKem Gold, buffered with 150 mM HEPES at pH 7.4) (Figure 2). The bone position was adjusted to obtain the calcification at the interface between the bone and the hydrogel. The chamber was connected to the double diffusion system and the solutions were flowing at a rate of $0.0052 cm^3/s$ for 7 days. Five samples were used as control (without teZCC) and five samples with teZCC were obtained.

**2.3.3 Micro-computed tomography scan—**The presence of the calcification was evaluated using a micro-CT scanner (Skyscan 1076, Kontich, Belgium). At day 7, directly after being removed from the double diffusion system, bone–hydrogel constructs were imaged using the following parameters: 9 μm resolution, 49 kV voltage source, 200 μA current, Al 0.5 mm filter.

**2.3.4 Experimental push-off test—**Following the imaging analysis, the hydrogel was prepared so that 3 mm remained above the bone. Pushoff test (Figure 3(A)) was performed by immobilising the bone and applying a downward uniaxial displacement at 0.5 mm/s on the hydrogel while measuring the load (Mach-1™ V500, BioSyntech, Montreal, QC, Canada). The indenter was positioned at 1 mm from the bone–hydrogel interface. This gap ensured that the indenter did not enter in contact with the bone. The peak load was defined as the force before failure and the interfacial shear strength was defined as the peak load divided by the interface surface. Finally, the energy to failure per surface was defined as the area under the load–displacement curve until failure normalised by the interface surface (Figure 3(B)).

**2.3.5 Numerical push-off model—**This model replicated the experimental push-off test (Figure 1(B)). The construct had the same geometry and material properties as in the ones of the osteochondral defect model (Table 1). A paired contact condition with default penalty factor, relative to the material properties, was imposed between the indenter and the hydrogel, to prevent the indenter to penetrate the hydrogel. The indenter was positioned 1

mm (*z*-direction) from the bone interface to match the experimental condition. The bone was fixed and a downward uniaxial displacement imposed by the indenter was applied on the hydrogel. The displacement corresponded to the maximal one experienced by the samples at failure during the experimental tests. The corresponding reaction forces on the indenter were predicted. The peak load, interfacial shear strength and energy to failure were defined as for the experimental push-off tests. The numerical model was solved by Comsol 4.2 with MUMPS solver and quadratic triangles elements.

The meshing was set as 'fine', but it was verified that results did not significantly change compared to a more refined meshing.

### 2.4 Statistics

Experimental and numerical data were presented as mean ± SEM. The effect of teZCC in experimental measurements and numerical predictions was evaluated by *t*-test. Differences were considered significant for $P < 0.05$.

## 3. Results

### 3.1 Numerical osteochondral defect model

Under compression, due to the Poisson effect, a lateral displacement of the host cartilage was observed (Figure 4). The maximal lateral displacement of cartilage was about 0.1 mm. This displacement created a lateral force, which induced a shear stress at the interface between the hydrogel and the bone. The shear stress along the interface was moderate and similar for construct with or without teZCC (Figure 5(A)). However, close to the construct–host tissue interface ($z = 3$ mm), the shear stress profile changed in the hydrogel. Without the teZCC, the implanted construct endured an increase of shear stress at the hydrogel–bone interface to a maximum of 800 kPa (Figure 5(B)). The presence of teZCC kept the shear stress to a maximum of 20 kPa at the teZCC–hydrogel interface (Figure 5(B)). The osteochondral defect model showed then that the presence of the teZCC helps to lower the interfacial shear stress.

### 3.2 Experimental push-off test

An hydrogel–bone construct with a teZCC of about 0.5 mm in thickness was obtained (Figure 6(A)). The mineral presence was confirmed by micro-CT images (Figure 6(B)). Peak load, interfacial shear strength and energy to failure per area were statistically higher for construct with teZCC (Figure 7(A) and Table 2). Failures occurred at the teZCC–hydrogel interface. The zone of calcification stayed attached to the bone after the push-off test, and the teZCC–bone interface was located inside the bone sample (Figure 6(B)).

### 3.3 Numerical push-off test model

The results obtained with the numerical push-off tests model were consistent with the experimental values of peak load, interfacial shear strength and energy to failure per area (Table 2). For the same displacements to failure obtained experimentally (1 ± 0.1 mm), the numerical model predicted an increase in the shear strength in construct with the teZCC (Figure 7(B)). The good agreement between numerical and experimental data suggests that

the mechanical effect of the teZCC is adequately captured with the proposed numerical model.

## 4. Discussion

A strong attachment of a soft structure to a rigid material is usually difficult to obtain due to the mismatch of the corresponding mechanical properties. For the natural osteochondral tissue, the negative effect of this mismatch in mechanical properties is attenuated with the presence of a calcified interface between the cartilage and the bone. The *in vitro* formation of a calcified interface between a hydrogel and a bone could then be a potentially interesting strategy in the development of an artificial osteochondral construct. In this study, biomechanical evaluations of this strategy were performed.

One of the important results obtained with the numerical osteochondral defect model was to clarify the shear phenomena at the construct interface between the hydrogel and the bone. This shear stress was induced by the lateral expansion of the loaded host cartilage. Shear stresses can also be induced at the cartilage–ZCC interface or hydrogel–teZCC interface during compression due to the attachment of cartilage or hydrogel to the underlying rigid calcified region (Radin et al. 1991). Since the lateral spread is restrained by this fixation, a shear stress is produced, adding to that induced by the expansion of the host cartilage. The incorporation of a calcified interface in the numerical model served to substantially lower the induced shear stress. The reduction in shear stress value is certainly related to the creation of a gradient of mechanical properties due to the calcified interface as observed in general at the interface of materials presenting very different mechanical properties (Yang and Temenoff 2009). Based on the developed numerical osteochondral defect model, there is a clear advantage to experimentally induce a calcification between the hydrogel and a piece of bone in the development of an artificial osteochondral construct.

Several methods have been developed to control *in vitro* calcification. A cell-mediated technique was proposed using β-glycerophosphate during deep zone chondrocyte cell culture (Hwang et al. 2010). In this work, we have adapted a technique based on a double diffusion system (Boskey 1989; Hunter et al. 1996) to control the calcification at an interface between a gel and a piece of bone. This method allowed for a fast calcification as shown by the presence of a calcified interface between the hydrogel and bone in 7 days. This duration is particularly shorter than a calcification induced by cells (Kandel et al. 1997). The calcification was confirmed through μCT imaging. The calcification zone allowed to significantly increase the anchorage of the hydrogel in bone, as demonstrated by a 100% peak load increase during push-off tests compared to the situation without calcified interface. This result may be analogous to those of previous studies where calcification was induced by cells (Allan et al. 2007; St-Pierre et al. 2012). While the obtained calcified interface did not allow attainment of peak loads typical of a cartilage bone interface (Lima et al. 2008), the corresponding increase in shear strength could still present a biomechanical advantage for the initial anchorage of the hydrogel in bone.

The numerical osteochondral defect model highlighted that shear stress is an important variable to consider during osteochondral construct deformation. It is worth mentioning that

the biomechanical evaluation of the calcified interface through push-off test is therefore a relevant functional test for the osteochondral construct. The numerical push-off test model furnished values in accordance with the experimental push-off test data validating then the numerical model for the osteochondral construct.

The numerical models presented several limitations. As proposed in previous numerical studies (Lima et al. 2004; Kelly and Prendergast 2006; D'Lima et al. 2009; Vahdati and Wagner 2011), the boundary conditions for the osteochondral defect model were simplified as only compression were considered in quasi-static mode. While compression is the principal mode of cartilage loading (Peterson and Bronzino 2008; Andriacchi et al. 2009), we may not exclude that other loading conditions such as shear between the tibial and femoral cartilages would affect the calculated interfacial shear stress obtained between the hydrogel and the bone. The compression values used as boundary conditions were obtained from *in vivo* data (Liu et al. 2010).

In this study, we showed that the presence of a teZCC might increase the anchorage of a hydrogel to a bone within two phenomena. First, the calcified interface might directly increase the shear strength of the hydrogel anchorage in the bone. Second, by creating a gradient of mechanical properties, the calcified interface might decrease the shear stress at the hydrogel bone interface. Tissue engineering of the interface presents then an interesting complementary approach to increase the mechanical performances of construct made of soft and hard materials.

## Acknowledgments

This project (S-10-10P) was supported by the AO Research Fund of the AO Foundation. The authors thank to Karen Poon and Carmen Bonvin for their help during the writing process of this manuscript.

## References

Allan KS, Pilliar RM, Wang J, Grynpas MD, Kandel RA. Formation of biphasic constructs containing cartilage with a calcified zone interface. Tissue Eng. 2007; 13(1):167–177. [PubMed: 17518590]

Andriacchi TP, Koo S, Scanlan SF. Gait mechanics influence healthy cartilage morphology and osteoarthritis of the knee. J Bone Joint Surg Am. 2009; 91(Suppl 1):95–101. [PubMed: 19182033]

Boskey AL. Hydroxyapatite formation in a dynamic collagen gel system: effects of type I collagen, lipids, and proteoglycans. J Phys Chem. 1989; 93(4):1628–1633.

Broom ND, Oloyede A, Flachsmann R, Hows M. Dynamic fracture characteristics of the osteochondral junction undergoing shear deformation. Med Eng Phys. 1996; 18:396–404. [PubMed: 8818138]

Butz KD, Chan DD, Nauman EA, Neu CP. Stress distributions and material properties determined in articular cartilage from MRI-based finite strains. J Biomech. 2011; 44(15):2667–2672. [PubMed: 21920526]

Davis, JR. ASM International Handbook Committee. Stainless steels. Materials Park, OH: ASM International; 1994.

D'Lima DD, Chen PC, Colwell CW. Osteochondral grafting: effect of graft alignment, material properties, and articular geometry. Open Orthop J. 2009; 3:61–68. [PubMed: 19696917]

Emans PJ, Hulsbosch M, Wetzels GM, Bulstra SK, Kuijer R. Repair of osteochondral defects in rabbits with ectopically produced cartilage. Tissue Eng. 2005; 11(11–12):1789–1796. [PubMed: 16411824]

Ferguson VL, Bushby AJ, Boyde A. Nanomechanical properties and mineral concentration in articular calcified cartilage and subchondral bone. J Anat. 2003; 203:191–202. [PubMed: 12924819]

Grayson WL, Bhumiratana S, Grace Chao PH, Hung CT, Vunjak-Novakovic G. Spatial regulation of human mesenchymal stem cell differentiation in engineered osteochondral constructs: effects of pre-differentiation, soluble factors and medium perfusion. Osteoarthritis Cartilage. 2010; 18(5): 714–723. [PubMed: 20175974]

Hauch KN, Oyen ML, Odegard GM, Haut Donahue TL. Nanoindentation of the insertional zones of human meniscal attachments into underlying bone. J Mech Behav Biomed Mater. 2009; 2(4):339–347. [PubMed: 19627840]

Hollenstein, J.; Hwang, J.; Cory, E.; Pioletti, DP.; Sah, RL. Engineering a zone of calcification that is localized in space and mechanically stiff. Proceedings of the Transactions of the Orthopaedic Research Society; 2011; Long Beach, CA. 2011.

Hunter GK, Hauschka PV, Poole AR, Rosenberg LC, Goldberg HA. Nucleation and inhibition of hydroxyapatite formation by mineralized tissue proteins. J Biochem. 1996; 317(Pt 1):59–64.

Hwang J, Kyubwa EM, Bae WC, Bugbee WD, Masuda K, Sah RL. *In vitro* calcification of immature bovine articular cartilage: formation of a functional zone of calcified cartilage. Cartilage. 2010; 1(4):287–297. [PubMed: 22745850]

Kandel RA, Boyle J, Gibson G, Cruz T, Speagle M. *In vitro* formation of mineralized cartilagenous tissue by articular chondrocytes. In Vitro Cell Dev Biol Anim. 1997; 33:174–181. [PubMed: 9112125]

Kelly DJ, Prendergast PJ. Prediction of the optimal mechanical properties for a scaffold used in osteochondral defect repair. Tissue Eng. 2006; 12(9):2509–2519. [PubMed: 16995784]

Lima EG, Grace Chao PH, Ateshian GA, Bal BS, Cook JL, Vunjak-Novakovic G, Hung CT. The effect of devitalized trabecular bone on the formation of osteochondral tissue-engineered constructs. Biomaterials. 2008; 29(32):4292–4299. [PubMed: 18718655]

Lima EG, Mauck RL, Han SH, Park S, Ng KW, Ateshian GA, Hung CT. Functional tissue engineering of chondral and osteochondral constructs. Biorheology. 2004; 41(3–4):577–590. [PubMed: 15299288]

Liu F, Kozanek M, Hosseini A, Van de Velde SK, Gill TJ, Rubash HE, Li G. *In vivo* tibiofemoral cartilage deformation during the stance phase of gait. J Biomech. 2010; 43(4):658–665. [PubMed: 19896131]

Mente PL, Lewis JL. Elastic modulus of calcified cartilage is an order of magnitude less than that of subchondral bone. J Orthop Res. 1994; 12:637–647. [PubMed: 7931780]

Normand V, Lootens D, Amici E, Plucknett K, Aymard P. New insight into agarose gel mechanical properties. Biomacromolecules. 2000; 1:730–738. [PubMed: 11710204]

Oegema T Jr, Carpenter R, Hofmeister F, Thompson RC Jr. The interaction of the zone of calcified cartilage and subchondral bone in osteoarthritis. Microsc Res Technol. 1997; 37:324–332.

Peterson, DR.; Bronzino, JD. Biomechanics: principles and applications. Boca Raton: CRC Press; 2008.

Redler I, Mow VC, Zimny ML, Mansell J. The ultrastructure and biomechanical significance of the tidemark of articular cartilage. Clin Orthop Relat Res. 1975; 112:357–362. [PubMed: 1192647]

Schaefer D, Martin I, Jundt G, Seidel J, Heberer M, Grodzinsky A, Bergin I, Vunjak-Novakovic G, Freed LE. Tissue-engineered composites for the repair of large osteochondral defects. Arthritis Rheum. 2002; 46(9):2524–2534. [PubMed: 12355501]

St-Pierre JP, Gan L, Wang J, Pilliar RM, Grynpas MD, Kandel RA. The incorporation of a zone of calcified cartilage improves the interfacial shear strength between in vitro-formed cartilage and the underlying substrate. Acta Biomater. 2012; 8(4):1603–1615. [PubMed: 22222151]

St-Pierre JP, Pilliar RM, Grynpas MD, Kandel RA. Calcification of cartilage formed *in vitro* on calcium polyphosphate bone substitutes is regulated by inorganic polyphosphate. Acta Biomater. 2010; 6(8):3302–3309. [PubMed: 20188870]

Vahdati A, Wagner DR. Finite element study of a tissue-engineered cartilage transplant in human tibiofemoral joint. Comput Methods Biomech Biomed Eng. 2011

Wiltsey C, Kubinski P, Christiani T, Toomer K, Sheehan J, Branda A, Kadlowec J, Iftode C, Vernengo J. Characterization of injectable hydrogels based on poly(N-isopropylacrylamide)-g-chondroitin

sulfate with adhesive properties for nucleus pulposus tissue engineering. J Mater Sci: Mater Med. 2013

Yang P, Temenoff J. Engineering orthopedic tissue interfaces. Tissue Eng B Rev. 2009; 15(2):127–141.

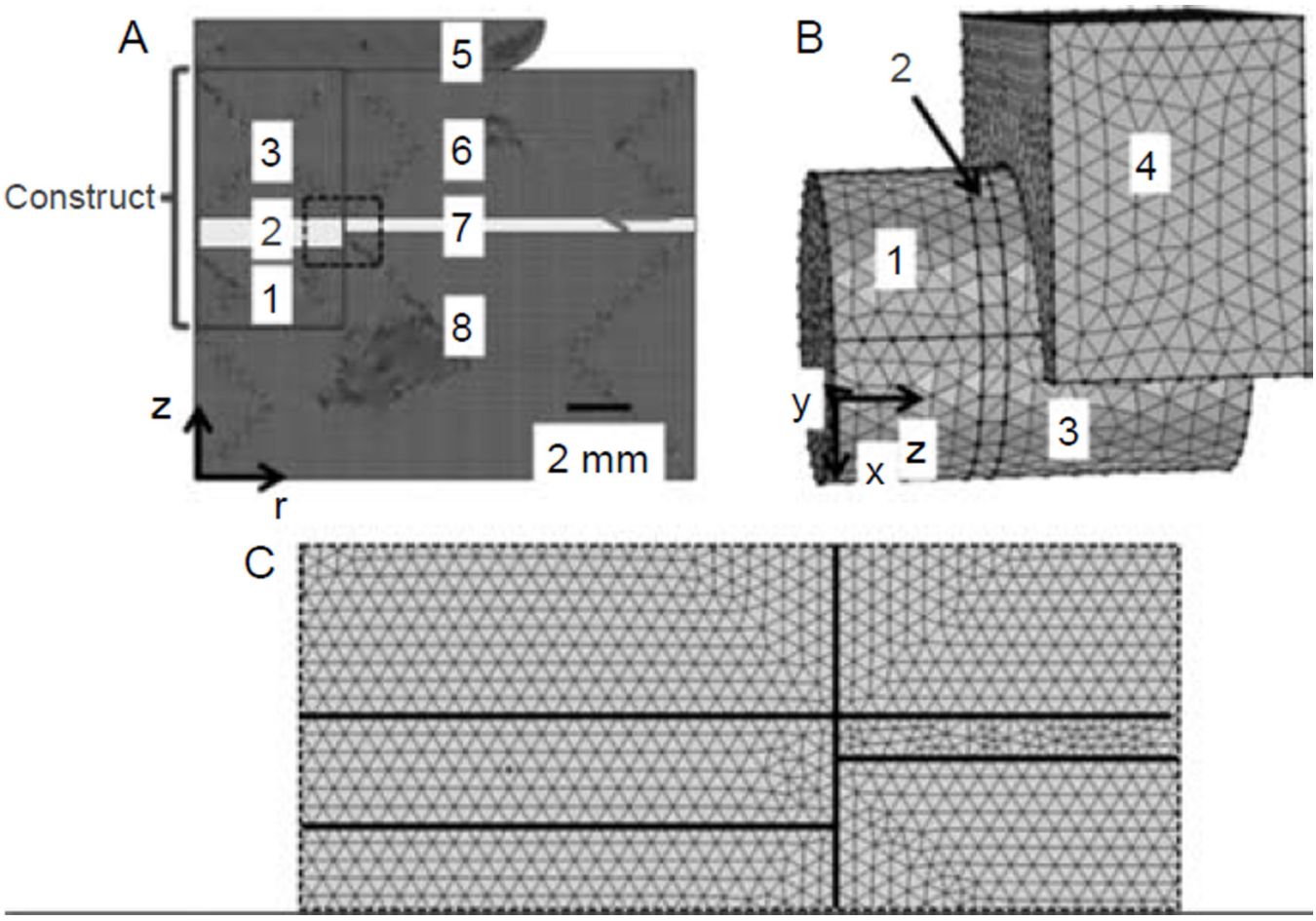


**Figure 1.**

Axisymmetric model of the osteochondral defect treatment (A) and (B) model of the push-off test. 1, Bone; 2, teZCC; 3, hydrogel; 4, indenter; 5, opposing host cartilage; 6, host cartilage; 7, host ZCC and 8, host bone. Red arrow highlights that the bottom of 3 and 7 are aligned. (C) Zoom of the black doted square detailing the mesh of the teZCC and ZCC.

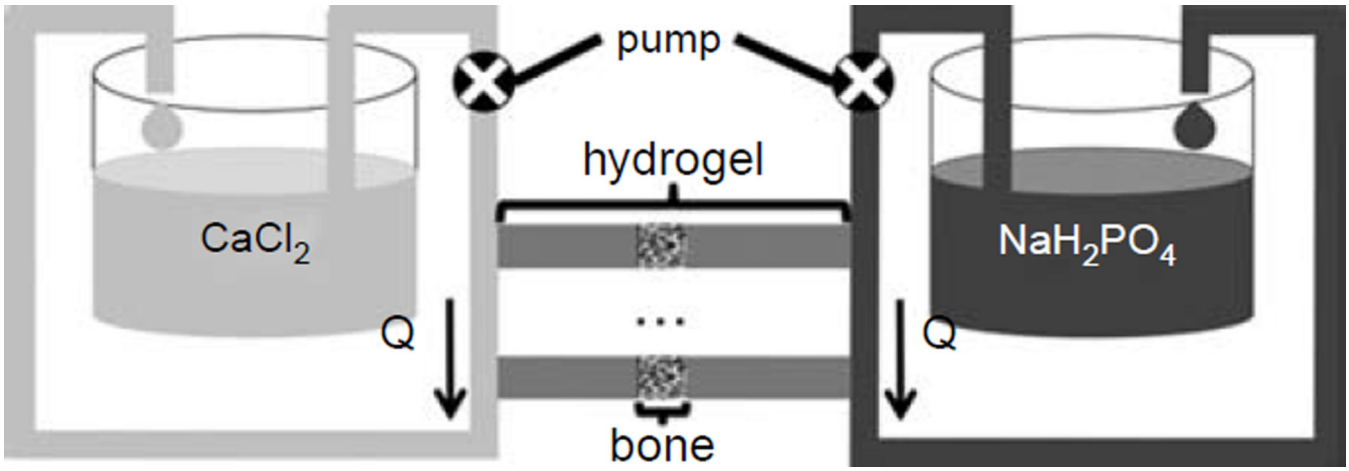


**Figure 2.**
Double diffusion system with the trabecular bone sample infiltrated with agarose hydrogel adapted from our previous study (Hollenstein et al. 2011). Calcium and phosphate solutions are circulating from each end of the hydrogel with the help of a peristaltic pump.

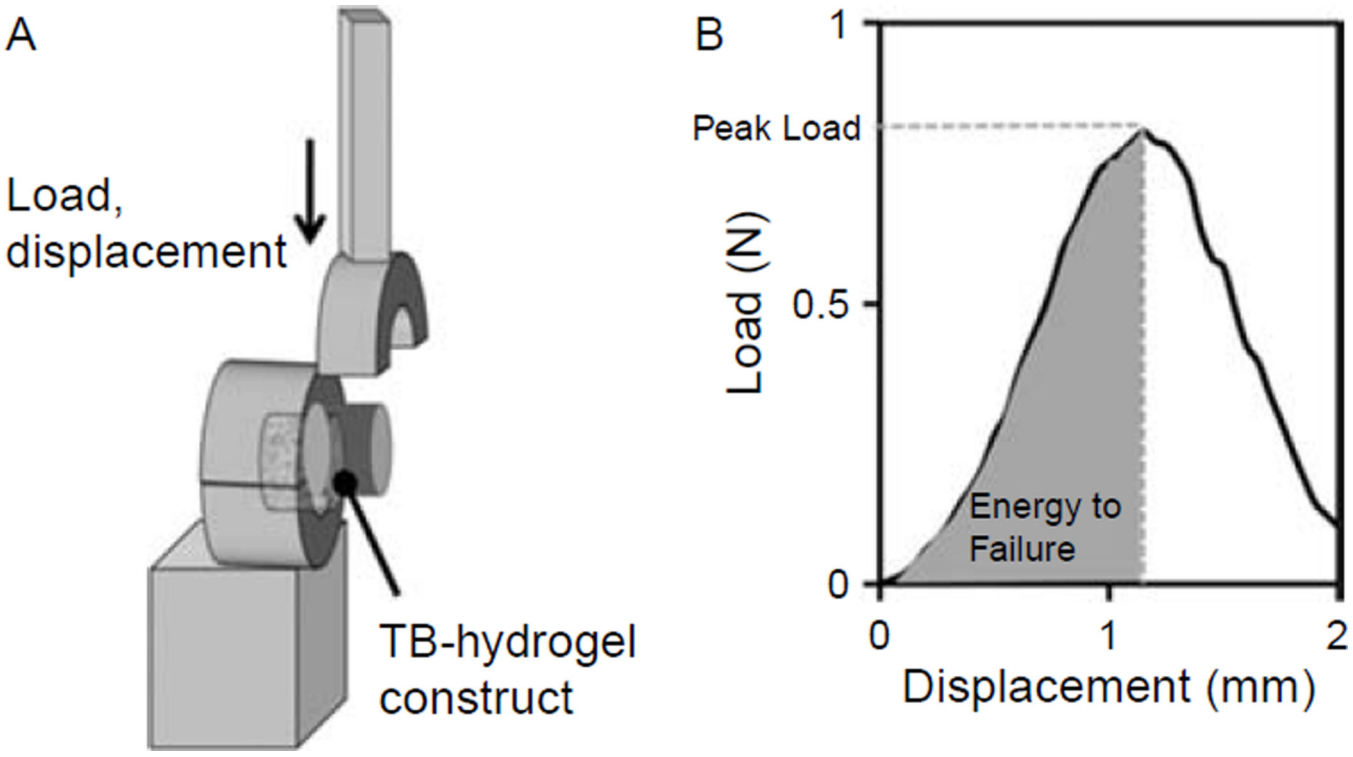


**Figure 3.**
Schematic of the push-off setup (A) and experimental results (B).

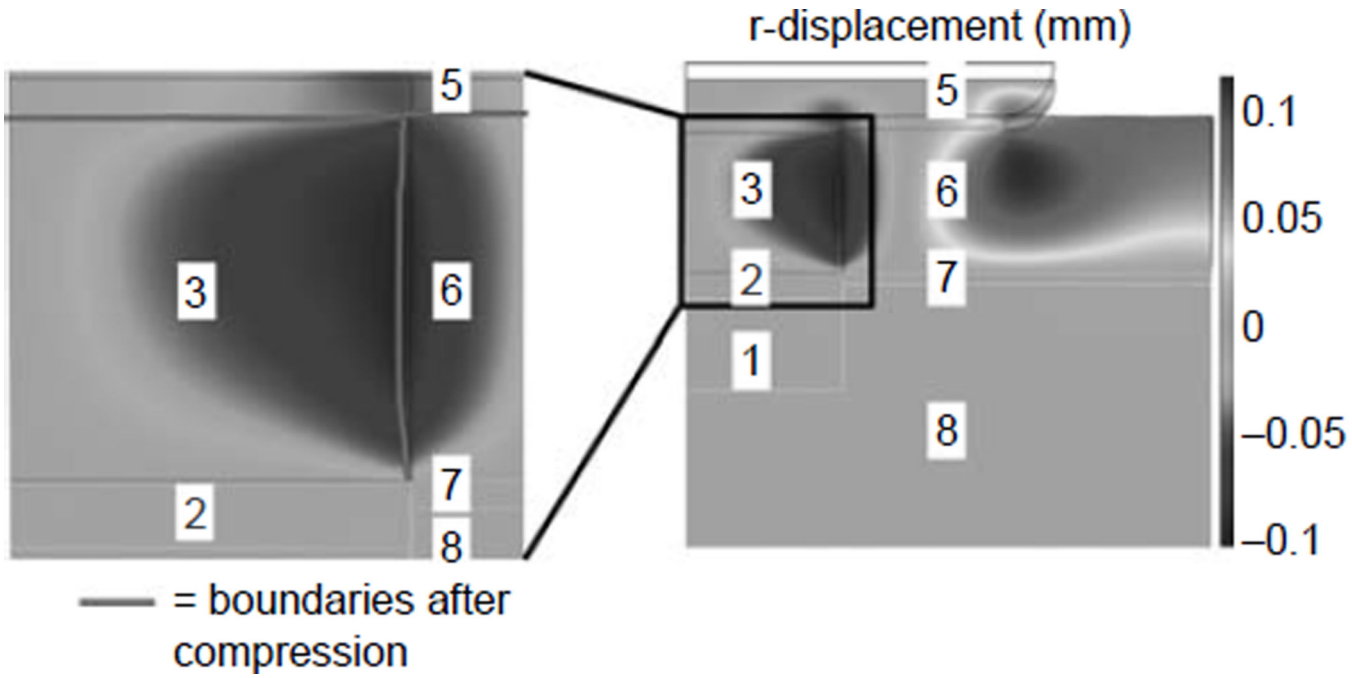


**Figure 4.**

Lateral expansion of the host cartilage following the 30% compression from the opposite host cartilage in the osteochondral defect treatment model. 1, Bone; 2, teZCC; 3, hydrogel; 5, opposing host cartilage, 6, host cartilage, 7, host ZCC and 8, host bone.

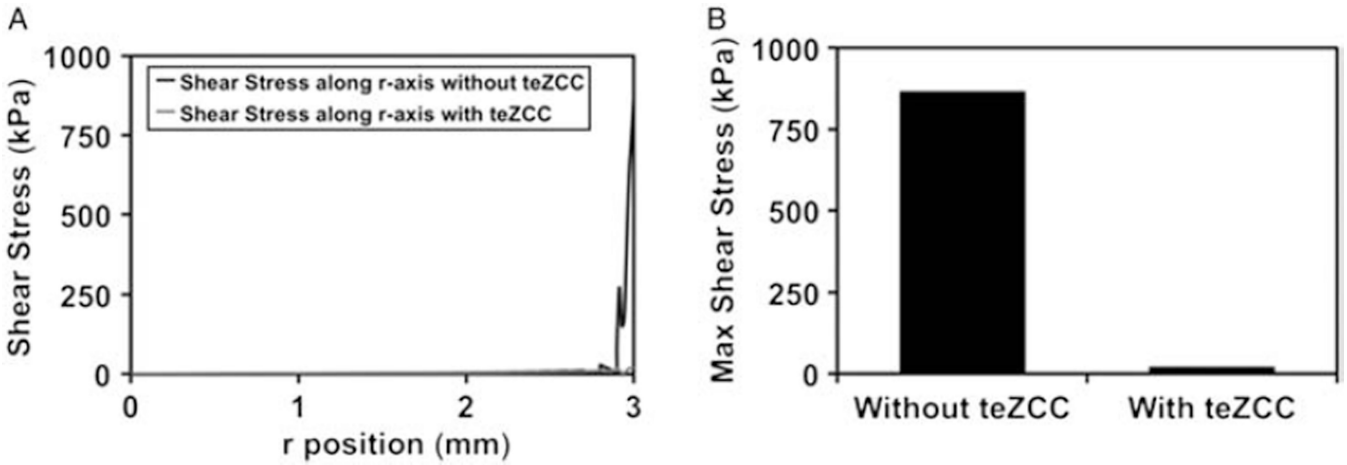


**Figure 5.**

Shear stress along bone–hydrogel interface axis (without teZCC) and along teZCC–hydrogel interface axis (with teZCC) at 30% compression in the osteochondral defect treatment model (A). Maximum shear stress (B).

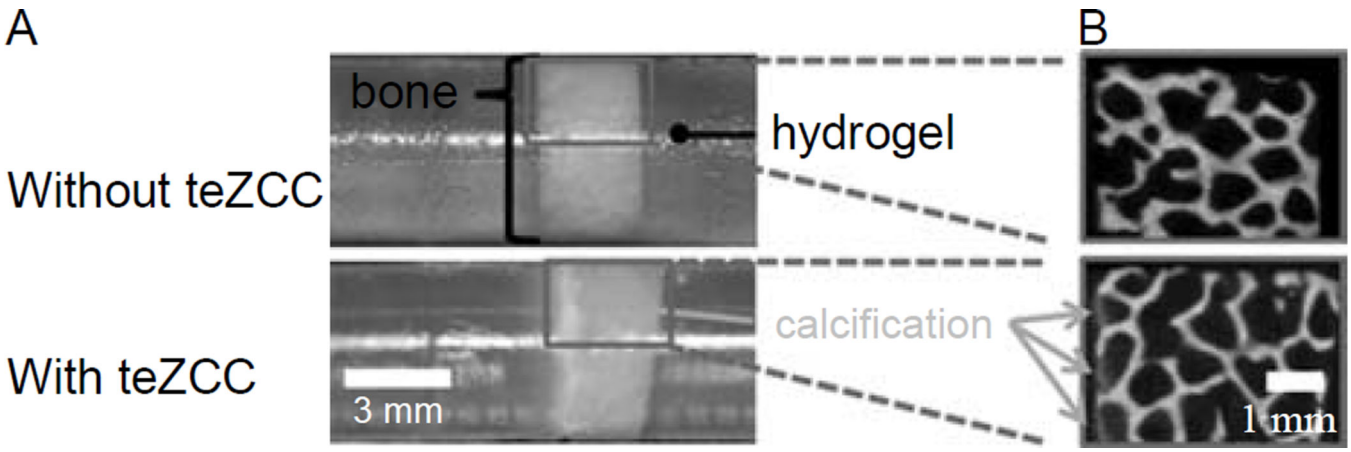


**Figure 6.**
Photography of a control sample and calcified sample after 7 days (A). Micro-CT image at 9 μm resolution (B).

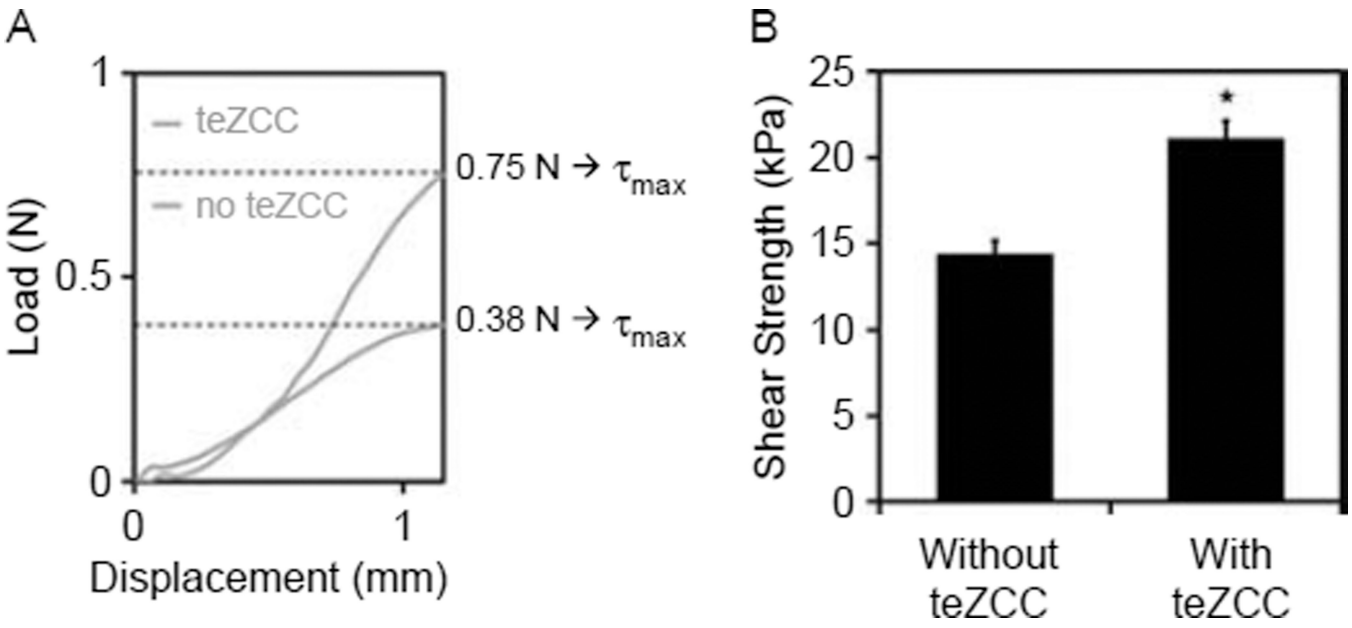


**Figure 7.**
Push-off test. Typical experimental load–displacement curve (A). Numerical shear strength with and without teZCC at failure displacements (B) (*$P < 0.05$).

**Table 1**

Material properties used in the two models.

| Tissue | Material/zone | Thickness | *E* modulus | Poisson ratio | References |
|---|---|---|---|---|---|
| Indenter | 316 Stainless Steel | 3 mm | 196 GPa | 0.3 | Davis (1994) |
| Construct | Hydrogel | 3 mm | 0.16 MPa | 0.45 | Hollenstein et al. (2011) and Normand et al. (2000) |
| | teZCC | 0 or 0.5 mm | 1.5 MPa | 0.3 | Hollenstein et al. (2011) |
| | Trabecular bone | 3 mm | 1 GPa | 0.3 | Lima et al. (2004) |
| Host | Cartilage | 3 mm | 10 MPa | 0.45 | D' Lima et al. (2009) and Kelly and Prendergast (2006) |
| | ZCC | 0.2 mm | 320 MPa | 0.3 | Mente and Lewis (1994) |
| | Bone | 5 mm | 6 GPa | 0.3 | Kelly and Prendergast (2006) and Mente and Lewis (1994) |

## Table 2

Comparison of experimental and numerical results.

| | Experimental | | Model | |
|---|---|---|---|---|
| | **Without teZCC** | **With teZCC** | **Without teZCC** | **With teZCC** |
| Peak load (N) at exp. failure displacement | 0.38 ± 0.04 | 0.74 ± 0.04* | 0.46 ± 0.03 | 0.69 ± 0.03* |
| Interfacial shear strength (kPa) | 11.96 ± 1.20 | 22.92 ± 0.60* | 14.34 ± 0.82 | 21.52 ± 0.94* |
| Energy to failure per area ($J/m^2$) | 7.40 ± 0.91 | 12.58 ± 1.32* | 6.87 ± 0.72 | 12.36 ± 1.09* |

Note:

*$P < 0.05$.